THERMODYNAMIC FUNCTIONS OF PENDULAR MOLECULES

Břetislav FRIEDRICH and Dudley R. HERSCHBACH

Department of Chemistry,
Harvard University, 12 Oxford St., Cambridge, MA 02138, U.S.A.

Received May 28, 1993
Accepted June 9, 1993

We dedicate this paper to Professor Otto Wichterle, with profound admiration for his great contributions to science, his steadfast leadership, and his legendary humanity.

External electric or magnetic fields can *hybridize* rotational states of individual dipolar molecules and thus create *pendular states* whose field-dependent eigenproperties differ qualitatively from those of a rotor or an oscillator. The pendular eigenfunctions are *directional*, so the molecular axis is *oriented*. Here we use quantum statistical mechanics to evaluate ensemble properties of the pendular states. For linear molecules, the partition function and the averages that determine the thermodynamic functions can be specified by two reduced variables involving the dipole moment, field strength, rotational constant, and temperature. We examine a simple approximation due to Pitzer that employs the classical partition function with quantum corrections. This provides explicit analytic formulas which permit thermodynamic properties to be evaluated to good accuracy without computing energy levels. As applications we evaluate the high-field average orientation of the molecular dipoles and field-induced shifts of chemical equilibria.

For dipolar molecules in low J states, the rotational motion often can be arrested by external electric or magnetic fields of feasible strength[1,2]. Instead of tumbling end-over-end, the molecules then become trapped in *pendular states*, with the molecular axis confined to librate over a limited angular range about the field direction. In this way substantial *spatial orientation* of the molecular axis can be attained for the lowest pendular states. These states exhibit sui generis features that can be observed spectroscopically, including field-dependent eigenenergies and marked intensity variations among transitions governed by the *directional* eigenfunctions.

Pendular orientation of polar molecules in electric fields is applicable to linear, symmetric and asymmetric top rotors; thus this method greatly surpasses in chemical scope the electric field focusing technique, which is limited to symmetric tops[3]. Magnetic pendular states can be obtained in analogous fashion for many molecules with nonzero electronic orbital momentum[4]. This includes large classes of molecules not accessible to the electric technique, particularly paramagnetic *nonpolar* molecules and molecular *ions*.

The characteristic features of pendular states have been demonstrated in prototype spectroscopic experiments[5 - 9] and employed to study reactions of oriented molecules[1,10]. Since pendular states can be created for individual molecules, pendular orientation is not limited to molecular systems out of equilibrium. This contrasts with most other techniques for producing anisotropic distributions of either the figure axis or the angular momentum of molecules. Ensemble properties of pendular molecules thus can be described by means of equilibrium quantum statistical mechanics. In this paper we give such a treatment and discuss some prospective applications.

Some Properties of Pendular States

For simplicity we consider a linear molecule without electronic angular momentum, but the chief results can be extended to other categories by standard means. The eigenenergies of the field-free rotor states $|J, M\rangle$ are given by

$$E_J = BJ(J+1), \tag{1}$$

where B is the rotational constant, J is the total angular momentum quantum number, and M the projection on the space-fixed Z-axis. By virtue of the different orientations of the $\boldsymbol{J}$-vector, these energy levels are $(2J+1)$-fold degenerate. Pendular states are coherent superpositions or hybrids of the field-free rotor states, created in response to the interaction between a dipole moment directed along the molecular axis and an external field. The interaction potential is given by

$$V(0)/B = -\omega \cos 0 \tag{2}$$

in units of the rotational constant, where 0 is the angle between the molecular dipole moment μ and the direction of the field and $\omega \equiv \mu\mathcal{F}/B$ is the dimensionless interaction parameter, with $\mathcal{F}$ the strength of the external field, whether electric, $\mathcal{E}$, or magnetic, $\mathcal{H}$.

The pendular states, $|\tilde{J}, M; \omega\rangle$, are labelled by the good quantum number M and the nominal value of $\tilde{J}$, the angular momentum of the field-free rotor state that adiabatically correlates with the high-field hybrid function, $|\tilde{J}, M; \omega \to 0\rangle \to |J, M\rangle$. For fixed values of $\tilde{J}$ and M the pendular state depends solely on the interaction parameter ω which determines the range of J involved in the hybrid wavefunction. Figure 1 summarizes these features in terms of a correlation diagram between the field-free rotor states ($\omega \to 0$) and the harmonic librator states ($\omega \to \infty$). For large ω, the pendulum eigenstates become increasingly directional with energies that differ greatly from the rotor levels. In the harmonic limit ($\omega \to \infty$) the levels become $(N+1)$-fold degenerate with eigenenergies

$$E_N = B[-\omega + (N+1)(2\omega)^{1/2}], \tag{3}$$

where $N = 2\tilde{J} - |M|$ is the total number of the librator quanta; $\tilde{J} - |M|$ is the number of 0-nodes (in the range 0° – 180°) and $|M|$ the number of φ-nodes (in 0° – 360°). Figure 2 shows for $\omega = 5$ the typical pattern of energy levels, in contrast to the free-rotor and harmonic librator limits. Qualitatively, the lowest states within the cosine potential well are libratorlike whereas those appreciably above the barrier top ($\theta \sim \pm 180°$) become rotor-like.

The Pendular Partition Function

We consider a canonical ensemble of molecules and as usual take the translational, electronic, vibrational, and rotational or pendular modes of motion as separable (although the Born–Oppenheimer approximation is somewhat less accurate in the presence of a strong field). For a given mode of molecular motion at temperature T, if Boltzmann statistics applies the occupation number n_i of the i-th energy level with energy E_i above the ground level E_0 and degeneracy g_i is given by

$$\frac{n_i}{n} = g_i \frac{\exp[-(E_i - E_0)/kT]}{Q}, \tag{4}$$

where

$$Q = \sum_{i=0}^{\infty} g_i \exp[-(E_i - E_0)/kT] \tag{5}$$

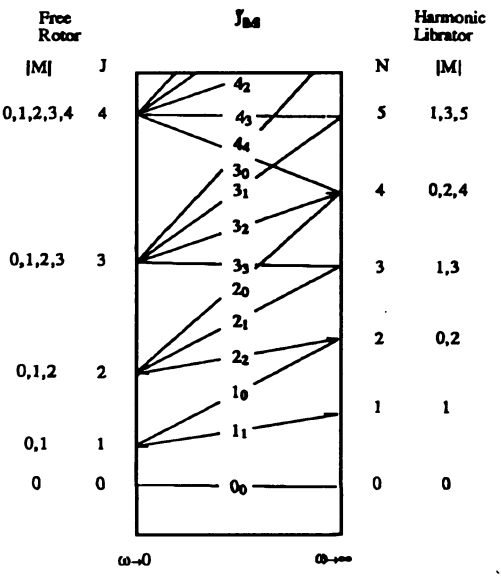

FIG. 1
Correlation diagram between field-free ($\omega = 0$) rotational states $|J, M\rangle$ for a linear molecule, specified in Eq. (*1*), and high-field ($\omega \to \infty$ limit) angular harmonic librator states $|N, M\rangle$, specified in Eq. (*3*)

is the canonical molecular partition function pertaining to the given mode and n is the total number of molecules in the ensemble possessing that mode. In general, for the pendular mode the exact partition function of Eq. (5) must be evaluated numerically, since as seen in Fig. 2 the spacing of the energy levels is not simple except in the free-rotor and harmonic librator limits. However, since the energy levels for any field strength are proportional to the rotational constant B, the partition function and related quantities depend only on a reduced temperature, $\gamma = kT/B$, in addition to the reduced interaction parameter, $\omega = \mu\mathcal{F}/B$.

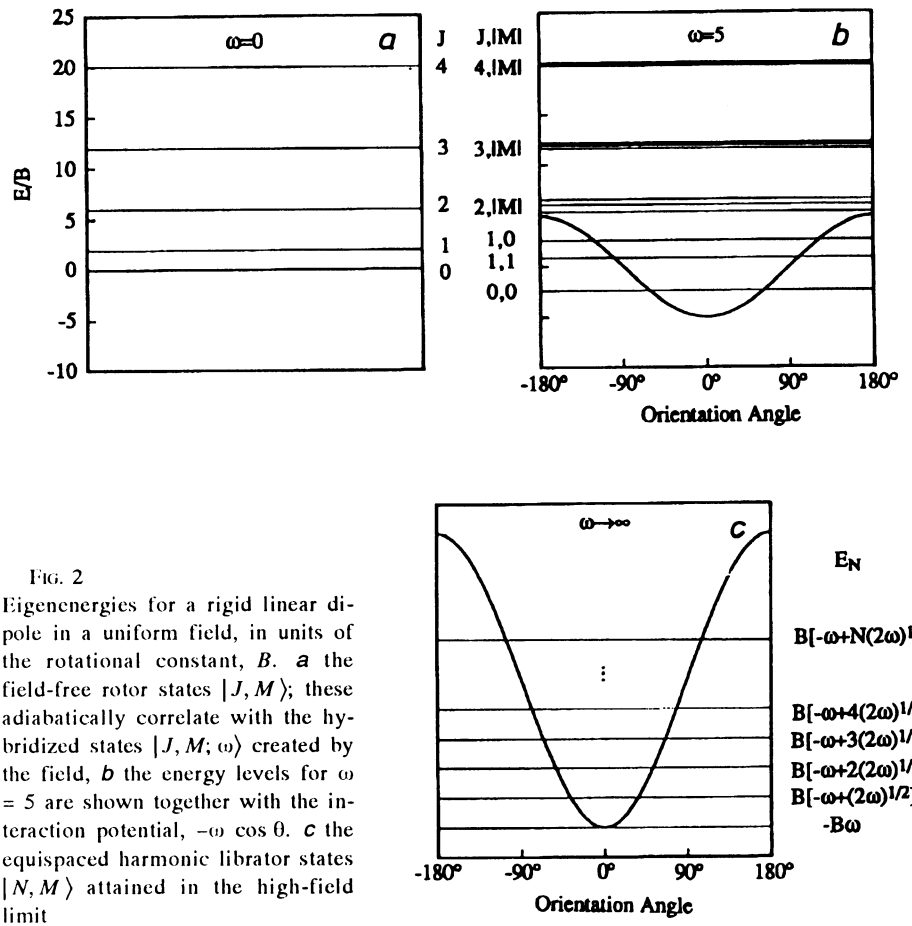

FIG. 2
Eigenenergies for a rigid linear dipole in a uniform field, in units of the rotational constant, B. *a* the field-free rotor states $|J, M\rangle$; these adiabatically correlate with the hybridized states $|J, M; \omega\rangle$ created by the field, *b* the energy levels for $\omega = 5$ are shown together with the interaction potential, $-\omega \cos\theta$. *c* the equispaced harmonic librator states $|N, M\rangle$ attained in the high-field limit

Figure 3 shows $Q(\omega,\mathcal{Y})$ for $\omega = 0$, 5, 20, and 100 as determined from computations using a program that generates the pendular eigenenergies[7]. For the field-free case ($\omega = 0$), corresponding to Eq. (*1*), the partition function is simply that for a rigid linear rotor,

$$Q_{\mathrm{rot}}(\mathcal{Y}) = \sum_{J=0}^{\infty} (2J + 1) \exp[-J(J + 1)/\mathcal{Y}] . \qquad (6)$$

In the high-field or harmonic librator limit ($\omega \to \infty$), corresponding to Eq. (*3*), the partition function becomes that for an isotropic two-dimensional oscillator with frequency $B(2\omega)^{1/2}$; thus

$$Q_{\mathrm{lib}} = \sum_{N=0}^{\infty} (N + 1)\, \mathrm{e}^{-Nu} = (1 - \mathrm{e}^{-u})^{-2} , \qquad (7)$$

where $u \equiv (2\omega)^{1/2}/\mathcal{Y}$. At a given temperature, the presence of the field is seen to reduce the partition function markedly below that for a free rotor, but except in certain regions (ω large but $\mathcal{Y}$ not too large) it differs substantially from that for a harmonic librator.

Since the population of the ground state is related to the partition function by $n_0 = n/Q$, we see from Fig. 3 that at a given temperature n_0 grows as ω increases and the energy levels are drawn further apart. Because the lowest rotational states are hybridized most easily, such "condensation" of molecules into the low-lying states occurs at field-strengths substantially lower than those required to attain the harmonic librator limit.

We find that a simple procedure utilizing the classical limit as well as Q_{rot} and Q_{lib} provides a remarkably accurate analytic approximation for the complete partition func-

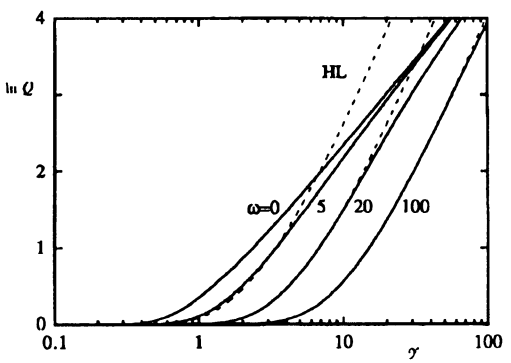

FIG. 3
Total partition functions $Q(\omega,\mathcal{Y})$ determined from Eq. (*5*) for pendular mode (full curves), as functions of reduced temperature $\mathcal{Y} = kT/B$ for four values of reduced interaction strength, $\omega = \mu\mathcal{F}/B$. The field-free limit ($\omega = 0$) pertains to the rotational partition function Q_{rot} of Eq. (*6*); the high-field limit (dashed curves) to the harmonic librator (HL) function Q_{lib} of Eq. (*7*). By virtue of the logarithmic ordinate scale, these plots also show the negative of the Helmholtz free energy function, $-F/RT$; cf. Table I

tion. This procedure, introduced by Pitzer in treating hindered internal rotation[11], recasts the partition function as the product of three factors:

$$Q(\omega, \gamma) = [Q_{\mathrm{rot}}]_{\mathrm{cl}} \left[\frac{Q}{Q_{\mathrm{rot}}}\right]_{\mathrm{cl}} \left[\frac{Q_{\mathrm{q}}}{Q_{\mathrm{cl}}}\right]_{\mathrm{lib}} . \qquad (8)$$

These factors enable a neat separation of variables: the first factor is independent of the field and depends only on $\gamma = kT/B$; the second factor depends only on the ratio $\omega/\gamma = \mu\mathcal{F}/kT$; the third to a very good approximation only on $u = (2\omega)^{1/2}/\gamma$. Furthermore, explicit analytic expressions are readily obtained for each of the three factors. Hence the partition function and thermodynamic properties can be evaluated to good accuracy without actually determining the field-dependent eigenenergies or computing the sums called for in Eq. (5). We consider the three factors in turn.

The field-free factor, $[Q_{\mathrm{rot}}]_{\mathrm{cl}}$, is the classical limit of the rotational partition function of Eq. (6), given by

$$[Q_{\mathrm{rot}}]_{\mathrm{cl}} = (2\pi IkT/h^2)\, 4\pi = kT/B = \gamma , \qquad (9)$$

where h is Planck's constant and I the moment of inertia, related to the rotational constant by $B = \hbar^2/2I$, with $\hbar = h/2\pi$.

The second factor, $[Q/Q_{\mathrm{rot}}]_{\mathrm{cl}}$, is the field-dependent portion of the classical partition function. The classical counterpart of Eq. (5) takes the form

$$Q_{\mathrm{cl}} = \frac{Q_{\mathrm{f}}}{4\pi} \int_0^{2\pi} \mathrm{d}\varphi \int_0^{\pi} \mathrm{e}^{-\alpha(1-\cos\vartheta)} \sin\vartheta \,\mathrm{d}\vartheta . \qquad (10)$$

Here for brevity we denote by Q_{f} the field free portion, given in Eq. (9). In the Boltzmann factor of Eq. (10), the potential energy of Eq. (2) is replaced by $\omega(1 - \cos\vartheta)$, in

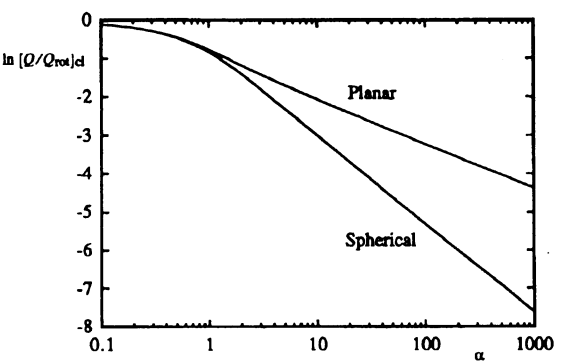

FIG. 4
Field-dependent portion of classical partition function for a spherical pendulum, given by Eq. (11), as a function of the ratio $\alpha = \omega/\gamma = \mu\mathcal{F}/kT$. Also shown is the corresponding plot for a planar pendulum

order to refer the energy zero to the potential minimum, as appropriate for the classical case. The integral is given explicitly by

$$\frac{Q_{cl}}{Q_f} = \frac{e^{-\alpha} \sinh \alpha}{\alpha} \tag{11}$$

as a function of the ratio $\alpha \equiv \omega/\gamma = \mu\mathcal{J}/kT$. Figure 4 plots this function, which approaches unity as $\alpha \to 0$ and approaches $1/(2\alpha)$ as $\alpha \to \infty$. Included for comparison is the corresponding result for the planar pendulum case, for which $Q_f = (\pi\gamma)^{1/2}$ and $Q_{cl}/Q_f = e^{-\alpha} I_0(\alpha)$, with I_0 the modified Bessel function. The planar pendulum, solvable in terms of Mathieu functions, has long been employed in treating hindered internal rotation in molecules[12] as well as an approximate model for the interaction of rotating molecules with an electric field[2,13].

The third factor, $[Q_q/Q_{cl}]_{lib}$, serves to correct the classical version of the partition function for the effects of quantization. For this we find it is a very good approximation to use the ratio of Q_{lib} for the harmonic librator, as given in Eq. (7), to its classical limit ($u \to 0$). Accordingly, the correction factor is simply Γ^2, where

$$\Gamma = \frac{u}{1 - e^{-u}} . \tag{12}$$

Figure 5 displays a test of the approximation. The ratio of the exact quantum partition function from Fig. 3 (for ω = 5, 20, 100) to the classical version from Eq. (10) is seen

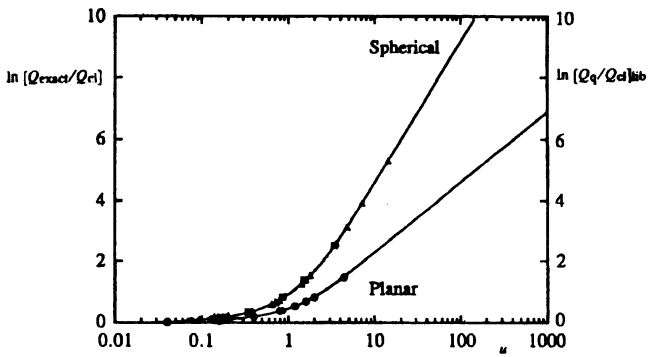

FIG. 5

Points give ratio of exact partition function for a spherical pendulum, as calculated from Eq. (5) for potential of Eq. (2), to the classical partition function from Eq. (10), for ω = 5 (■), 20 (▲), and 100 (◆); full curve gives quantum correction factor Γ^2 computed for harmonic librator from Eq. (12). Corresponding points for a planar pendulum were obtained from tables of Pitzer and Gwinn[12], and compared with correction factor Γ for a one-dimensional harmonic oscillator

to depend essentially only on u and to agree closely with Γ^2, the librator ratio. Similar agreement obtains for the planar pendulum, for which the correction factor is just Γ, in accord with the tests provided by Pitzer and Gwinn[12] in terms of thermodynamic functions. Although Q_{lib} is not a good approximation to the partition function for either a spherical or a planar pendulum, except for large values of u (cf. Fig. 3), the quantum/classical ratio for the quadratic librator potential mimics very well that for the cosine potential almost over the full range. The exception occurs for very low values of the reduced temperature, $\gamma < 1$, when both $\alpha \to \infty$ and $u \to \infty$; then the librator ratio becomes much too large. In practice, this is not a significant limitation, since such low values of γ very seldom obtain.

We note two other instructive aspects of Pitzer's procedure. The quantum partition function of Eq. (*5*) and the classical version of Eq. (*10*) employ different origins for the energy scales, respectively the lowest level and the potential minimum. The correction ratio of Eq. (*12*) automatically takes account of this difference because in $\ln \Gamma$ the leading term as $u \to 0$ is $u/2$; that has just the effect of shifting the energy zero from the lowest quantum level to the bottom of the potential curve[14]. Also, at low temperatures (low γ) the quantum rotational partition function differs appreciably from the classical value of Eq. (*9*). A correction for this can be made by inserting in Eq. (*8*) another factor, the ratio of the quantum Q_{rot} to its classical limit. Unless ω is zero or much smaller than γ, however, such a correction is not warranted. When ω is appreciable, the correction ratio derived from the librator limit, Γ^2 for the spherical case or Γ for the planar case, simulates the net effect of quantization for both the bound and unbound states of the cosine potential (cf. Fig. 2) and fully accounts for the pendular degree(s) of freedom.

The Thermodynamic Functions

Since the Helmholtz free energy F, internal energy U, entropy S, and heat capacity C are derived from the logarithm of the partition function[15], the factorization provided by Eq. (*8*) gives the contributions of the pendular mode to all such functions Φ as a sum of three terms, each dependent on a single dimensionless reduced variable:

$$\Phi = \Phi_I(\gamma) + \Phi_{II}(\alpha) + \Phi_{III}(u) . \qquad (13)$$

Table I lists these terms. The thermodynamic functions are as usual per mole rather than per molecule, so the gas constant R appears (rather than Boltzmann's constant k). As the function pertain to a nominal ideal gas, the Gibbs free energy is given by $G = F + RT$, the enthalpy by $H = U + RT$, and the heat capacities at constant pressure and volume are related by $C_p = C_v + R$. The contribution from the pendular mode thus is the same for G and F, for H and U, and for either heat capacity.

For convenience, we list the conversion factors relating the physical parameters in customary units to our dimensionless variables. With temperature in K, rotational constant B in cm^{-1}, electric dipole moment $\mu_{\mathcal{E}}$ in Debye units and electric field strength $\mathcal{E}$ in kV/cm, or magnetic dipole moment $\mu_{\mathcal{H}}$ in Bohr magnetons and magnetic field strength $\mathcal{H}$ in Tesla units (= 10 kGauss), we have:

$$\gamma = 0.6961T/B$$

$$\omega_{\mathcal{E}} = 0.0168\,\mu_{\mathcal{E}}\mathcal{E}/B$$

$$\omega_{\mathcal{H}} = 0.4668\,\mu_{\mathcal{H}}\mathcal{H}/B \qquad (14)$$

with $\alpha = \omega/\gamma$ and $u = (2\omega)^{1/2}/\gamma$.

Figure 3 illustrates the field-dependence of the Helmholtz free energy, as $-F/RT = \ln Q$. The results obtained from the Pitzer procedure of Eqs (*8*) and (*13*) coincide with our numerical calculations employing Eq. (*5*) within the width of the plotted curves. Figures 6 – 8 show corresponding results for the internal energy, entropy, and heat capacity. In the presence of the field, the free energy and heat capacity increase, the internal energy and entropy decrease. Table II gives the leading terms for expansions that describe the field-induced changes for small ω or large γ. For sizable ω values, the transition from dominantly librational motion at low temperatures to largely rotational

TABLE I
Thermodynamic functions, $\Phi(\omega,\gamma) = \Phi_{I}(\gamma) + \Phi_{II}(\alpha) + \Phi_{III}(u)$

$\Phi(\omega,\gamma)$	$\Phi_{I}(\gamma)$	$\Phi_{II}(\alpha)$	$\Phi_{III}(u)$
$\frac{F}{RT} = -\ln Q$	$-\ln\gamma$	$-\ln\left[\frac{\sinh\alpha}{\alpha}\right] + \alpha$	$-2\ln\left[\frac{u}{1-e^{-u}}\right]$
$\frac{U}{RT} = T\frac{\partial \ln Q}{\partial T}$	1	$1 - \alpha\coth\alpha + \alpha$	$2\left(\frac{u}{e^{-u}-1} - 1\right)$
$\frac{S}{R} = \frac{U-F}{RT}$	$1 + \ln\gamma$	$\ln\left[\frac{\sinh\alpha}{\alpha}\right] + 1 - \alpha\coth\alpha$	$2\ln\left[\frac{u}{1-e^{-u}}\right] + 2\left(\frac{u}{e^{-u}-1} - 1\right)$
$\frac{C}{R} = \frac{\partial}{\partial T}\left(T^2\frac{\partial \ln Q}{\partial T}\right)$	1	$1 - \alpha^2\left(\coth^2\alpha - 1\right)$	$2\left[\frac{u^2e^u}{\left(e^u-1\right)^2} - 1\right]$
$\omega = \mu\mathcal{F}/B$	$\gamma = kT/B$	$\alpha = \omega/\gamma$	$u = (2\omega)^{1/2}/\gamma$

motion at higher temperatures is evident in all the thermodynamic functions, but becomes most striking in the prominent bumps that appear in the temperature dependence of the internal energy and heat capacity.

Previous discussions of quantum statistical mechanics for molecules subject to electric or magnetic fields go back to Debye[16] and Van Vleck[17] but have been limited to the weak-field case, corresponding to a quadratic Stark or Zeeman effect. The partition function is then near the classical limit, and the results are essentially equivalent to those including just the terms up through order α^2 in our Table II. By means of the Pitzer procedure, however, it proves easy to attain good accuracy for the full range of interaction strengths.

TABLE II
Weak-field expansions of thermodynamic functions

$\frac{\Delta F}{RT}$	$\alpha - \frac{\alpha^2}{6}\left(1 - \frac{\alpha^2}{30} + \ldots\right)$	$-2\left(\frac{u}{2} - \frac{u^2}{24} + \ldots\right)$
$\frac{\Delta U}{RT}$	$1 - \frac{\alpha^3}{3}\left(1 - \frac{\alpha^2}{15} + \ldots\right)$	$-2\left(\frac{u}{2} - \frac{u^2}{12} + \ldots\right)$
$\frac{\Delta S}{R}$	$1 - \alpha - \frac{\alpha^2}{6}\left(1 - \frac{\alpha^2}{10} + \ldots\right)$	$+2\left(\frac{u^2}{12} - \ldots\right)$
$\frac{\Delta C}{R}$	$\frac{\alpha^2}{3}\left(1 - \frac{\alpha^2}{5} + \ldots\right)$	$-2\left(\frac{u^2}{12} - \ldots\right)$

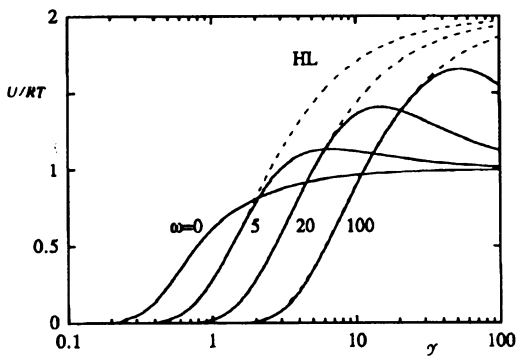

FIG. 6
Internal energy, U/RT, for a spherical pendulum as a function of reduced temperature, computed from Eq. (*13*) with factors listed in Table I, for ω = 0, 5, 20, and 100. Dashed curves show the harmonic librator (HL) limit. Figure 3 shows the corresponding curves for the Helmholtz free energy function, $-F/RT$

Although our treatment here is restricted to linear molecules without electronic angular momentum, we expect that more general cases can also be handled by augmenting standard methods with the Pitzer procedure. Often the classical partition function can be readily evaluated and separated into convenient factors[18] and the simple harmonic oscillator form for the quantum correction seems likely to be serviceable whenever the potential becomes quadratic in a suitable limit[12].

Ensemble Average of Molecular Orientation

The venerable Langevin–Debye function[16,17] describes the average orientation of a Boltzmann distribution of rotating rigid dipoles not interacting with each other but subject to an external field uniform in magnitude and direction. It corresponds to the classical limit of the partition function, which has been adequate for a host of experiments dealing with weak field-induced orientation, such as Kerr effect measurements. Quantum effects become substantial, however, in the strong-field, low-temperature regime explored in recent experiments[1 - 10]. Numerical calculations are straightforward but tedious since for large ω and small α many pendular eigenstates typically contribute. We find that Pitzer's method again proves useful; it provides an analytic approximation that surplants numerical computations for much of the range exhibiting marked quantum effects.

The orientation of the molecular dipole is specified by the expectation value of the cosine of the angle between the dipole axis and the field direction, $\langle \cos\theta \rangle$. According to the Hellman–Feynman theorem, this can be evaluated for a given state from the ω-dependence of the eigenenergy: $\langle \cos\theta \rangle_i = [-\partial(E_i/B)]/\partial\omega$. In general the derivative

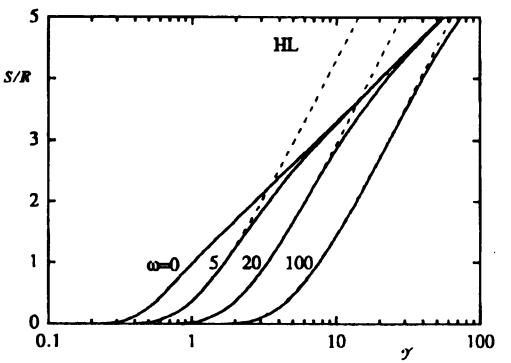

FIG. 7
Entropy, S/R, for a spherical pendulum as a function of reduced temperature, computed from Eq. (*13*) with factors listed in Table I, for ω = 0, 5, 20, and 100. Dashed curves show the harmonic librator (HL) limit

must be computed numerically, but for the harmonic librator limit ($\omega \to \infty$) we obtain from Eq. (3) a simple result,

$$\langle \cos 0 \rangle_N = 1 - \frac{N+1}{(2\omega)^{1/2}} . \tag{15}$$

The ensemble average, $\langle\langle \cos 0 \rangle\rangle$, of the orientation cosine for this limit then can be calculated from

$$\langle\langle \cos 0 \rangle\rangle = \sum_{N=0}^{\infty} \langle \cos 0 \rangle_N \frac{n_N}{n} , \tag{16}$$

where n_N is the occupation number of the N-th level, given by Eq. (4).

Hence

$$\langle\langle \cos 0 \rangle\rangle = 1 - \frac{(1 - e^{-u})^2}{(2\omega)^{1/2}} \sum_{N=0}^{\infty} (N+1)^2 e^{-Nu} . \tag{17}$$

The sum over the librator levels can be derived from a geometric series; with $x \equiv e^{-u}$, it is given by

$$\frac{d}{dx}\left[\frac{x}{(1-x)^2}\right] = \frac{(1+x)}{(1-x)^3} . \tag{18}$$

Thus we find for the ensemble average in the harmonic librator limit,

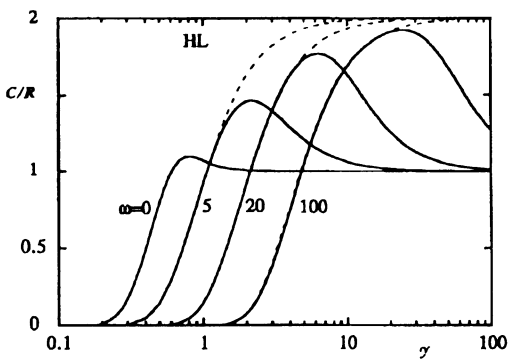

FIG. 8

Heat capacity, C/R, for a spherical pendulum as a function of reduced temperature, computed from Eq. (13) with factors listed in Table I, for ω = 0, 5, 20, and 100. Dashed curves show the harmonic librator (HL) limit

$$\langle\langle \cos\theta \rangle\rangle = 1 - \frac{\coth(u/2)}{(2\omega)^{1/2}} . \qquad (19)$$

This requires ω large but holds for any $\mathcal{Y}$; by letting $\mathcal{Y}$ grow such that $u \equiv (2\omega)^{1/2}/\mathcal{Y} \to 0$, we obtain the classical limit, where $\coth(u/2) \to 2/u$. The ratio of Eq. (*19*) to this limit is

$$\Gamma_\theta(\alpha, u) \equiv \frac{\alpha - (u/2)\coth(u/2)}{\alpha - 1} . \qquad (20)$$

We apply Pitzer's method by multiplying the classical ensemble average, given by the Langevin–Debye formula, by the Γ_θ-ratio and thereby have

$$\langle\langle \cos\theta \rangle\rangle = \left(\coth\alpha - \frac{1}{\alpha} \right) \Gamma_\theta(\alpha, u) . \qquad (21)$$

The correction factor $\Gamma_\theta < 1$, since for all $u > 0$ the quantity $(u/2)\coth(u/2) > 1$. However, our expression for Γ_θ is only adequate for ω large enough to enable α to substantially exceed both $(u/2)\coth(u/2)$ and unity. Elsewhere we simply set $\Gamma_\theta = 1$ or extrapolate smoothly to the Langevin–Debye curve. However, the latter is very well approximated by $(\alpha - 1)/\alpha$ for $\alpha > 2$, so coincides with the classical librator limit ($u \to 0$) there. In that range, Eq. (*21*) thus reduces simply to the quantum harmonic librator limit of Eq. (*19*).

Figure 9 displays this approximation for $\omega = 10, 20, 100$. The chief effect is simply a "rounding-off" of the Langevin–Debye result at large α. This rounding becomes less

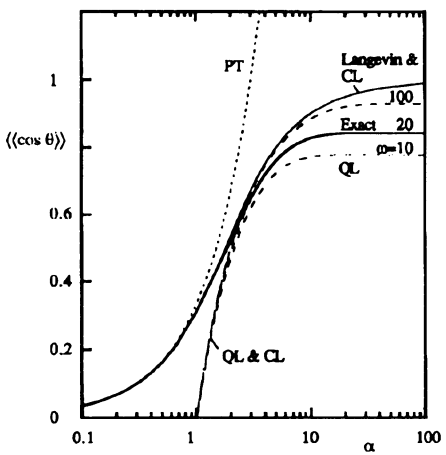

FIG. 9
Ensemble average of orientation cosine, $\langle\langle \cos\theta \rangle\rangle$, as a function of $\alpha = \mu\mathcal{F}/kT$, according to the classical Langevin–Debye formula with and without the approximate quantum correction of Eq. (*21*). Also shown are curves obtained from the second-order perturbation theory (PT, dotted) and from both quantum (QL) and classical (CL) versions of the harmonic librator limit (dashed), at $\omega = 10$, 20, and 100. A numerical calculation ("Exact") is also shown for $\omega = 20$; this coincides with Eq. (*21*) within the thickness of the plotted curve

pronounced as ω increases. We find agreement with numerical calculations is good for $\omega = 20$. The utility of Eq. (*21*) rapidly deteriorates for smaller ω, but in that range numerical calculations become less onerous.

Field-Induced Shifts of Chemical Equilibria

The factorization provided in Eq. (*8*) by the Pitzer approximation facilitates evaluating equilibrium constants for reactions of dipolar molecules in the presence of strong external fields. The equilibrium constant for a chemical reaction thus takes the form $K_0 K_y(\omega,\mathcal{Y})$, where K_0 denotes the constant that pertains in the absence of the field. The factor $K_y(\omega,\mathcal{Y})$ has the same form as the usual equilibrium product but with the partial pressure or concentration $[j]$ of each dipolar species replaced by

$$\mathcal{K}_j = \frac{e^{-\alpha_j} \sinh \alpha_j}{\alpha_j} \left(\frac{u_j}{1 - e^{-u_j}} \right)^2 . \qquad (22)$$

For each species that does not interact with the field, the $[j]$-factor is replaced by unity. Examples include three types of exchange reactions of diatomic molecules.

$$A + BC \leftrightarrow AB + C \qquad K_y = \mathcal{K}_{AB}/\mathcal{K}_{BC} \qquad (A)$$

$$A_2 + B_2 \leftrightarrow 2\,AB \qquad K_y = (\mathcal{K}_{AB})^2 \qquad (B)$$

$$AB + CD \leftrightarrow AC + BD \qquad K_y = \mathcal{K}_{AC}\mathcal{K}_{BD}/\mathcal{K}_{AB}\mathcal{K}_{CD} \qquad (C)$$

Type (*B*) is typically expected to exhibit the strongest field dependence, since in (*A*) and (*C*) the factors tend to balance out. In (*B*), since at a given temperature the free energy of the dipolar product AB increases, the reaction will be inhibited as ω increases. Figure 10 displays the functional dependence of the $K_y(\omega,\mathcal{Y})$ factor. For instance, the curve for $\omega = 10$ pertains to $I_2 + Cl_2 \leftrightarrow 2\,ICl$ at a field strength of about 50 kV/cm; the reduced temperature scale for ICl is such that the minimum of the curve (at $\mathcal{Y} \sim 5$) comes at about 1 K. Thus, field induced shifts of such equilibria are typically quite small. Such shifts can become significant if exceptionally low temperatures can be attained (perhaps for reactions occurring in a supersonic expansion) or exceptionally large ratios of μ/B (as for large, very polar molecules).

DISCUSSION

Our chief motivation has been to provide means to readily estimate thermodynamic properties for gas-phase molecules subject to strong external fields at relatively low temperatures. Both the method and results seem likely to find wider application. The simplicity and accuracy afforded by Pitzer's procedure, correcting the classical partition function by the harmonic oscillator ratio, recommended it for many problems involving strong perturbations. The results obtained here for pendular molecules are applicable also to condensed phase systems if interactions among the molecules are much less significant that with the external field.

The pendular functions may indeed even prove useful in modelling the effect of internal fields exerted by neighbors in a liquid or solid. The tumbling of a linear molecule in a condensed phase is more aptly represented by a spherical rather than a planar pendulum. At low temperatures or high density, the molecules in condensed phases are chiefly confined to librational or jostling motions, with occasional excursions to adjacent potential minima. This is much like hindered internal torsion within molecules such as ethane. The hindering potential barrier is not a constant, however, but depends on the orientation and density of packing of neighboring molecules. As the temperature is increased or density lowered, the jostling increasingly turns into tumbling. Heat capacity curves of molecular solids often show anomalies resembling the bumps seen in Fig. 8, although sometimes much sharper. These are usually attributed to a rather sudden transition from librational to rotational motion. The sharpening stems from the cooperative effect of the mutual rotation of neighboring molecules, which weakens the hindering potential and so makes the transition occur more abruptly. The cooperative behavior thus might be simulated by averaging over a range of the ω-parameter. In such ways, the easily evaluated pendular properties may serve to induce useful hybridization among treatments of many dynamical phenomena involving inhibiting but pliable barriers.

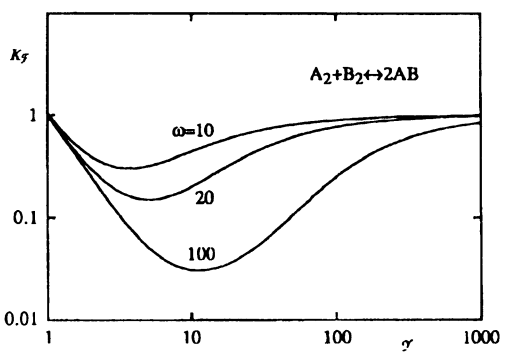

FIG. 10
Field-dependent portion of equilibrium constant K_γ for reactions of type (*B*) as a function of reduced temperature γ and reduced field strength ω = 10, 20, and 100

We are grateful for support of this work by the National Science Foundation.

REFERENCES

1. Loesch H. J., Remscheid A.: J. Chem. Phys. *94*, 4779 (1990); J. Phys. Chem. *95*, 8194 (1991).
2. Friedrich B., Herschbach D. R.: Z. Phys., D *18*, 153 (1991); Friedrich B., Pullman D. P., Herschbach D. R.: J. Phys. Chem. *95*, 8118 (1991).
3. For reviews, see Brooks P. R.: Science *193*, 11 (1976). Stolte S. in: *Atomic and Molecular Beam Methods* (G. Scoles, Ed.), Vol. I, Chap. 25; Oxford University Press, Oxford 1988. Parker D. H., Bernstein R. B.: Ann. Rev. Phys. Chem. *40*, 561 (1989).
4. Friedrich B., Herschbach D. R.: Z. Phys., D *24*, 25 (1992).
5. Friedrich B., Herschbach D. R.: Nature *353*, 412 (1991).
6. Block P. A., Bohac E. J., Miller R. E.: Phys. Rev. Lett. *68*, 1303 (1992).
7. Rost J.-M., Griffin J. C., Friedrich B., Herschbach D. R.: Phys. Rev. Lett. *68*, 1299 (1992).
8. Friedrich B., Rubahn H.-G., Sathyamurthy N.: Phys. Rev. Lett. *69*, 2487 (1992).
9. Friedrich B., Herschbach D. R., Rost J.-M., Rubahn H.-G., Renger M., Verbeek M.: J. Chem. Soc., Faraday Trans. 2 *89*, 1539 (1993).
10. Loesch H. J., Möller J.: J. Chem. Phys. *97*, 9016 (1992); J. Phys. Chem. *97*, 2158 (1993).
11. Pitzer K. S.: J. Chem. Phys. *5*, 469 (1937); *8*, 711 (1940).
12. Pitzer K. S., Gwinn W. D.: J. Chem. Phys. *10*, 428 (1942); Li J. C. M., Pitzer K. S.: J. Phys. Chem. *60*, 466 (1956).
13. Pauling L.: Phys. Rev. *36*, 430 (1930).
14. Pitzer K. S.: *Quantum Chemistry*, pp. 227, 325. Prentice–Hall, New York 1953.
15. Atkins P. W.: *Physical Chemistry* (W. H. Freeman, Ed.) p. 566, 4th ed. New York 1990.
16. Debye P.: *Polar Molecules*, pp. 27, 148. Dover, New York 1929.
17. Van Vleck J. H.: *The Theory of Electric and Magnetic Susceptibilities*, pp. 30, 181. Oxford, London 1932.
18. Herschbach D. R., Johnston H. S., Rapp D.: J. Chem. Phys. *31*, 1652 (1959).